

Figure 1.—A, Schematic geologic map of central California showing the distribution of terranes and other geological features in central California (modified after Murphy, 1983). The box outlines the area of figure 1B. B, Simplified geological map of central California west of the San Andreas fault, showing the location of the seismic-reflection profile, and the sources and receivers for the seismic-refraction profile.

INTRODUCTION

Seismic-reflection data from the Coast Ranges of central California were processed to extend the original 4-second Δ long record to 14 s. The seismic profile extends across the Coast Ranges of central California from the Pacific Coast near Morro Bay to the San Andreas fault. A seismic-refraction profile was also recorded from the Pacific Ocean to the foothills of the Sierra Nevada. The seismic-refraction profile extends from Morro Bay to the San Andreas fault. A comprehensive review of the geology of this region has been presented by Page (1984). The San Andreas fault is the boundary between the San Simeon (Franciscan assemblage-Stanley Mountain (ophiolite and Great Valley sequences) and the Salinian block (Mesozoic granitic rocks). A detailed description of the San Simeon-Stanley Mountain composite terrane and adjacent terranes is given by Murphy (1983). The Salinian block is a crystalline terrane containing closely spaced Cretaceous granitic plutons similar in age and composition to the rocks of the Sierra Nevada. The plutons in the Salinian block are older than the San Simeon plutons and are overlain by a sequence of Miocene and younger sedimentary rocks.

One motivation for reprocessing this data was to test whether a low-velocity zone in the lower crust, inferred to exist on the basis of large-offset data shot coincident with the reflection profile (Murphy and Costain, 1983), could be detected in the reflection data. In the large-offset data, a large-amplitude late arrival observed at 10 s was interpreted to be a wide-angle reflection from the base of a low-velocity zone having a vertical intercept time of about 8 s.

DATA ACQUISITION AND PROCESSING

The reflection data were shot and originally processed by Western Geophysical, Inc. in 1978 using the U.S. Geological Survey (USGS) seismic data processing program. A 48-channel, split-spread geometry was used with a station spacing of 67 m. The data were recorded with a sampling interval of 0.02 s and a nominal 24-fold coverage with a maximum offset of 1.8 km. Because most of the data were recorded with a 100 ms AGC, the data were filtered to define a smooth common depth point (CDP) line with a CDP spacing of 34 m and only accepted source receiver pairs for which the bottoming point coverage is quite variable (Fig. 2).

Twenty-four seconds of data were recorded from a 20-s Vibroseis sweep containing frequencies ranging from 16 to 32 Hz, yielding a 4-s record for each shot. The data were recorded in SEG-E format. The data were recorded in SEG-E format by the Society of Exploration Geophysicists in 1978. The data were collected with an upswep (a sweep in which frequency increases with time), it was possible to acquire a 8 s of data in 4 s. The data were collected with an upswep (a sweep in which frequency increases with time), it was possible to acquire a 14 s records, a method described by Okaya (1984). With this method, the high frequencies in the upswep were used to obtain a good reflection profile, and the low frequencies in the long fold sweep used in this experiment, a source frequency band of 24–32 Hz and only accepted source receiver pairs for which the bottoming point coverage is quite variable (Fig. 2).

In order to minimize the effect of spurious noise sources, such as passing vehicles, an AGC (automatic gain control) that had a window length of 100 ms was used. The AGC was used to remove the noise. The AGC has the effect of whitening the background noise in the correlated data (Corcoran and Costain, 1983). A sample of data was also processed without an AGC before reprocessing in order to preserve amplitude information.

After collecting the data, the data were sorted and reorganized at 8 s as normal moveout (NMO) corrected data. To eliminate the effect of the base of the basin was used as a reference. This greatly increased the continuity of reflectors and removed the effect of the dipping surface. A spherical divergence correction was applied to compensate for the effect of spherical spreading, and the data were pass-band filtered for the effect of normal moveout. The data were then converted to a linear interpolation of the two filters from 2 to 8 s. Experiments with the data showed that the data were not significantly improved in the data therefore, no deconvolution was applied for the final section.

Velocities for the normal moveout correction were determined for the upper 3–4 s from visual observation of the migration of the reflections. The data were sorted and reorganized to eliminate the effect of the dipping surface. The data were then converted to a linear interpolation of the two filters from 2 to 8 s. Experiments with the data showed that the data were not significantly improved in the data therefore, no deconvolution was applied for the final section.

After normal moveout, the data were muted and stacked. The stacked data were pass-band filtered (3–30 Hz) and AGC with a window length of 100 ms was used to remove the noise. The data were then migrated using a finite-difference algorithm. Both the unmigrated and migrated sections were converted to depth using a velocity model derived from both the reflection and refraction data.

DATA INTERPRETATION

Figure 4 shows the first 11.5 s of the full seismic section. No reflections were observed below 11.5 s. A line drawing interpretation is shown in Figure 5. The upper 3–4 s from visual observation of the migration of the reflections, and in places where no clear shallow reflectors could be observed, velocities suggested by the reflection data were used. The data were then converted to a linear interpolation of the two filters from 2 to 8 s. Experiments with the data showed that the data were not significantly improved in the data therefore, no deconvolution was applied for the final section.

The use of trade names is for descriptive purposes only and does not constitute endorsement by the U.S. Geological Survey.

of mafic. No deep reflections are seen beneath this region, probably at least in part due to the scattering or refraction of energy in the near surface.

Farther to the east, the sedimentary basin overlying the Salinian block is defined by the sedimentary rocks that have been tilted to a maximum of 25° (Fig. 4). These rocks show both normal and reverse faulting. The wedge-shaped region between the San Andreas fault and the eastern part of the Salinian block (km 45–60). These reflections are similar to those observed in several other reflection profiles across granitic batholiths reported to represent the base of the batholith (Murphy and others, 1984).

Most reflection and refraction data were shot beneath the Salinian block between 4 and 10 s and 10–20 s. The strength of these reflections is illustrated in Figure 7, in which amplitudes have been corrected only for spherical spreading and no AGC has been applied. Note the wedge-shaped region between the San Andreas fault and the eastern part of the Salinian block (km 45–60). These reflections are similar to those observed in several other reflection profiles across granitic batholiths reported to represent the base of the batholith (Murphy and others, 1984).

Twenty-four seconds of data were shot and originally processed by Western Geophysical, Inc. in 1978 using the U.S. Geological Survey (USGS) seismic data processing program. A 48-channel, split-spread geometry was used with a station spacing of 67 m. The data were recorded with a sampling interval of 0.02 s and a nominal 24-fold coverage with a maximum offset of 1.8 km. Because most of the data were recorded with a 100 ms AGC, the data were filtered to define a smooth common depth point (CDP) line with a CDP spacing of 34 m and only accepted source receiver pairs for which the bottoming point coverage is quite variable (Fig. 2).

Twenty-four seconds of data were recorded from a 20-s Vibroseis sweep containing frequencies ranging from 16 to 32 Hz, yielding a 4-s record for each shot. The data were recorded in SEG-E format. The data were recorded in SEG-E format by the Society of Exploration Geophysicists in 1978. The data were collected with an upswep (a sweep in which frequency increases with time), it was possible to acquire a 8 s of data in 4 s. The data were collected with an upswep (a sweep in which frequency increases with time), it was possible to acquire a 14 s records, a method described by Okaya (1984). With this method, the high frequencies in the upswep were used to obtain a good reflection profile, and the low frequencies in the long fold sweep used in this experiment, a source frequency band of 24–32 Hz and only accepted source receiver pairs for which the bottoming point coverage is quite variable (Fig. 2).

In order to minimize the effect of spurious noise sources, such as passing vehicles, an AGC (automatic gain control) that had a window length of 100 ms was used. The AGC was used to remove the noise. The AGC has the effect of whitening the background noise in the correlated data (Corcoran and Costain, 1983). A sample of data was also processed without an AGC before reprocessing in order to preserve amplitude information.

After collecting the data, the data were sorted and reorganized at 8 s as normal moveout (NMO) corrected data. To eliminate the effect of the base of the basin was used as a reference. This greatly increased the continuity of reflectors and removed the effect of the dipping surface.

A spherical divergence correction was applied to compensate for the effect of spherical spreading, and the data were pass-band filtered for the effect of normal moveout. The data were then converted to a linear interpolation of the two filters from 2 to 8 s. Experiments with the data showed that the data were not significantly improved in the data therefore, no deconvolution was applied for the final section.

Velocities for the normal moveout correction were determined for the upper 3–4 s from visual observation of the migration of the reflections. The data were sorted and reorganized to eliminate the effect of the dipping surface. The data were then converted to a linear interpolation of the two filters from 2 to 8 s. Experiments with the data showed that the data were not significantly improved in the data therefore, no deconvolution was applied for the final section.

After normal moveout, the data were muted and stacked. The stacked data were pass-band filtered (3–30 Hz) and AGC with a window length of 100 ms was used to remove the noise. The data were then migrated using a finite-difference algorithm. Both the unmigrated and migrated sections were converted to depth using a velocity model derived from both the reflection and refraction data.

ACKNOWLEDGMENTS

We thank Carl Wentworth for having made available the reflection data and John Miller, Dave Okaya and Myung Lee for advice on processing land reflection data.

We thank Carl Wentworth for having made available the reflection data and John Miller, Dave Okaya and Myung Lee for advice on processing land reflection data.

REFERENCES

Blumberg, C., and Prodeh, C., 1983, Crustal structure beneath the eastern part of the Coast Ranges of central California from seismic-refraction and new-surface-wave data: *Physics of the Earth and Planetary Interiors*, v. 31, p. 231–260.

Chambers, J., and Gromme, C.S., 1984, Paleomagnetic and geologic data indicating 2500 km of northward displacement for the Salinian block: *Geological Society of America Special Paper*, v. 245, p. 1–40.

Cochrane, C., and Okaya, T., 1984, Vela attenuation by Vibroseis white (VSW) processing: *Geophysics*, v. 49, no. 5, p. 543–554.

Lynn, R.B., Hale, L.D., and Thompson, G.A., 1981, Seismic refraction from the San Andreas fault zone, San Joaquin Valley, California: *Geophysical Research Letters*, v. 8, no. B1, p. 1053–1056.

McPhee, J., and Okaya, T., 1984, Data report for a seismic-refraction investigation—Morro Bay to the Sierra Nevada: U.S. Geological Survey Open-File Report 84-12, 12 plates.

Okaya, T., and Murphy, W., 1984, Reflection seismology—The San Andreas fault zone, San Joaquin Valley, California: *Geophysical Research Letters*, v. 11, no. 1, p. 239–242.

Okaya, T., and Murphy, W., 1987, Possible evidence for subducted sediments beneath central California: *Geology*, v. 15, no. 3, p. 254–256.

Wentworth, C.M., Walter, A.R., Barlow, J.A., and Zoback, M.D., 1983, Evidence for the tectonic origin of the San Joaquin Valley, California: Deep refraction and reflection profiles across the southeastern end of Kettleman Hill: *Bennett, J.L., and Sherburne, R.W., eds., The San Joaquin Valley, California: Geology and Resources*, U.S. Geological Survey Division of Mines and Geology Special Publication 65, p. 113–126.

* The use of trade names is for descriptive purposes only and does not constitute endorsement by the U.S. Geological Survey.

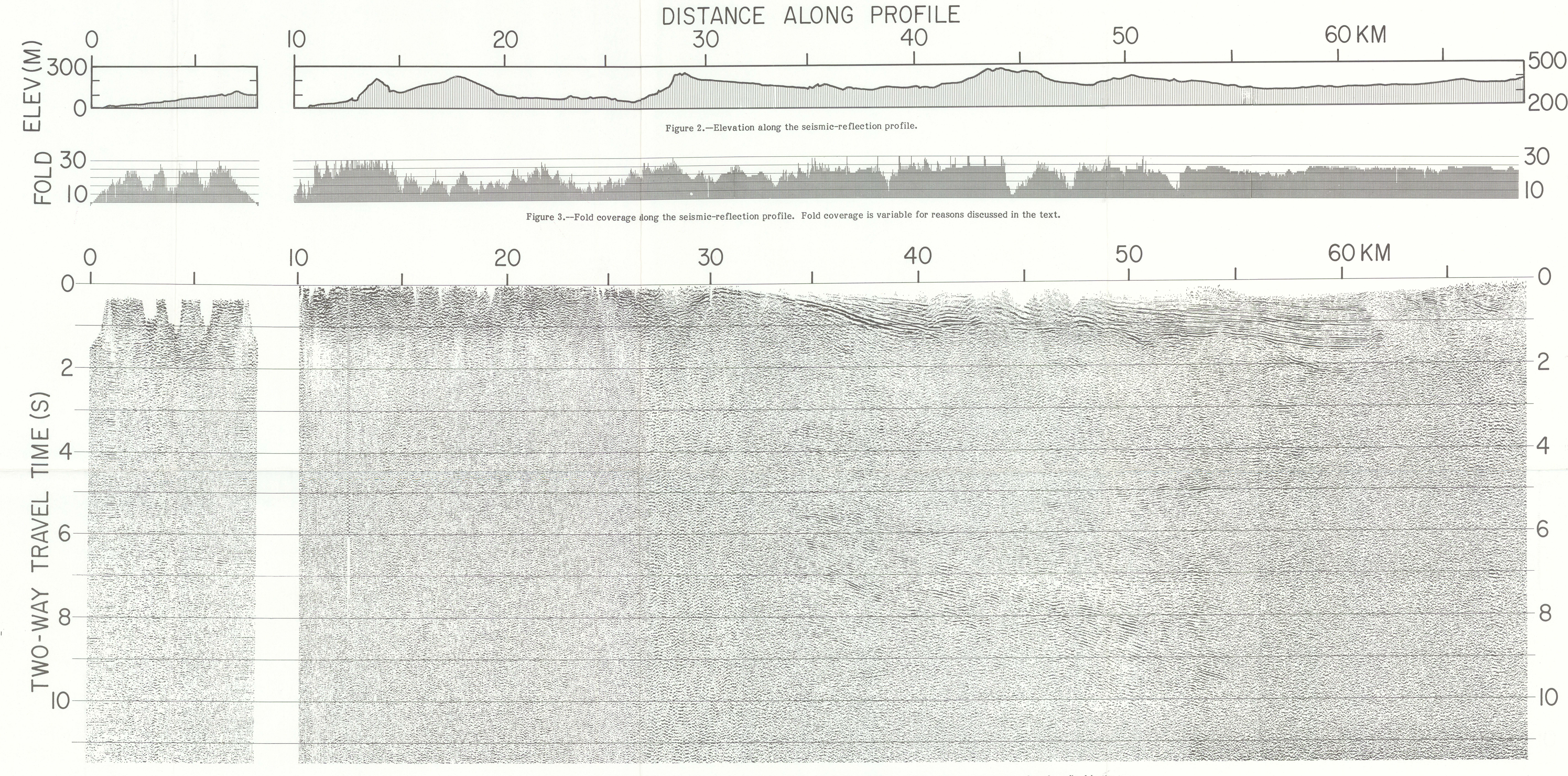


Figure 2.—Elevation along the seismic-reflection profile.



Figure 3.—Fold coverage along the seismic-reflection profile. Fold coverage is variable for reasons discussed in the text.

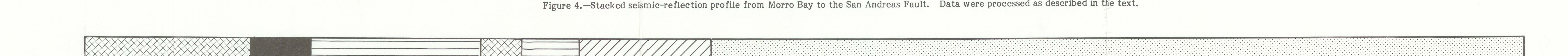


Figure 4.—Stacked seismic-reflection profile from Morro Bay to the San Andreas Fault. Data were processed as described in the text.

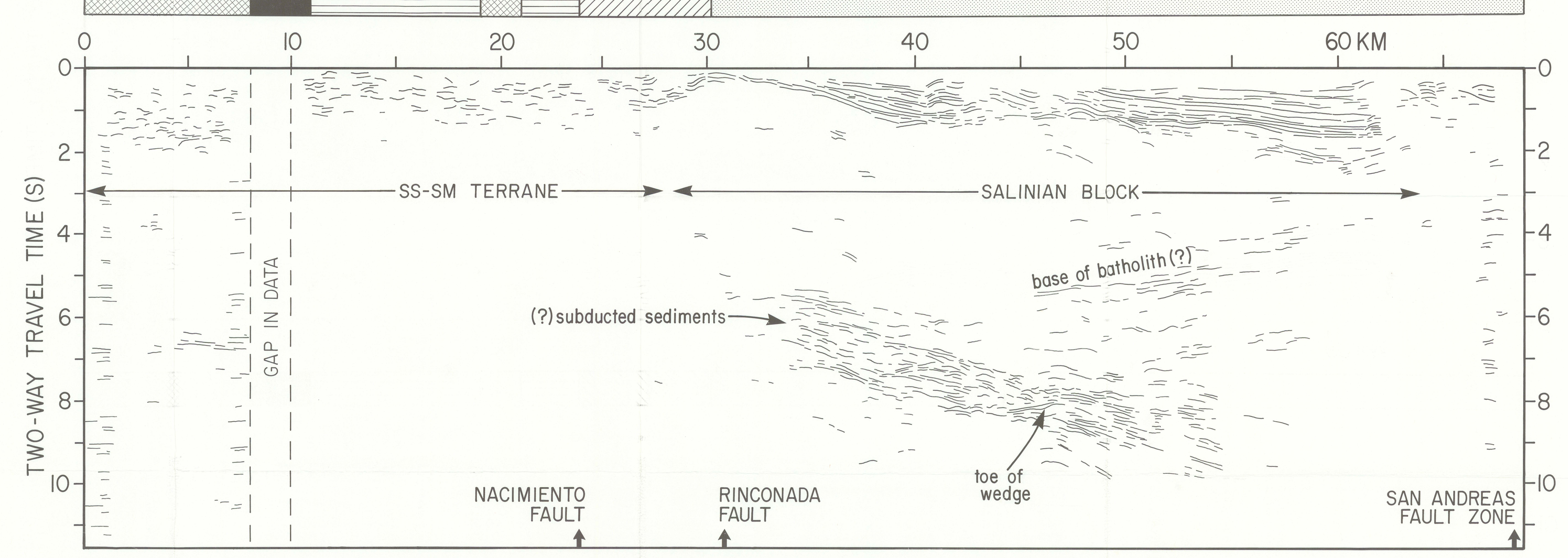


Figure 5.—Annotated line drawing of the seismic-reflection profile shown in figure 4 and bar graph of the surface geology (see figure 1B for explanation of patterns).

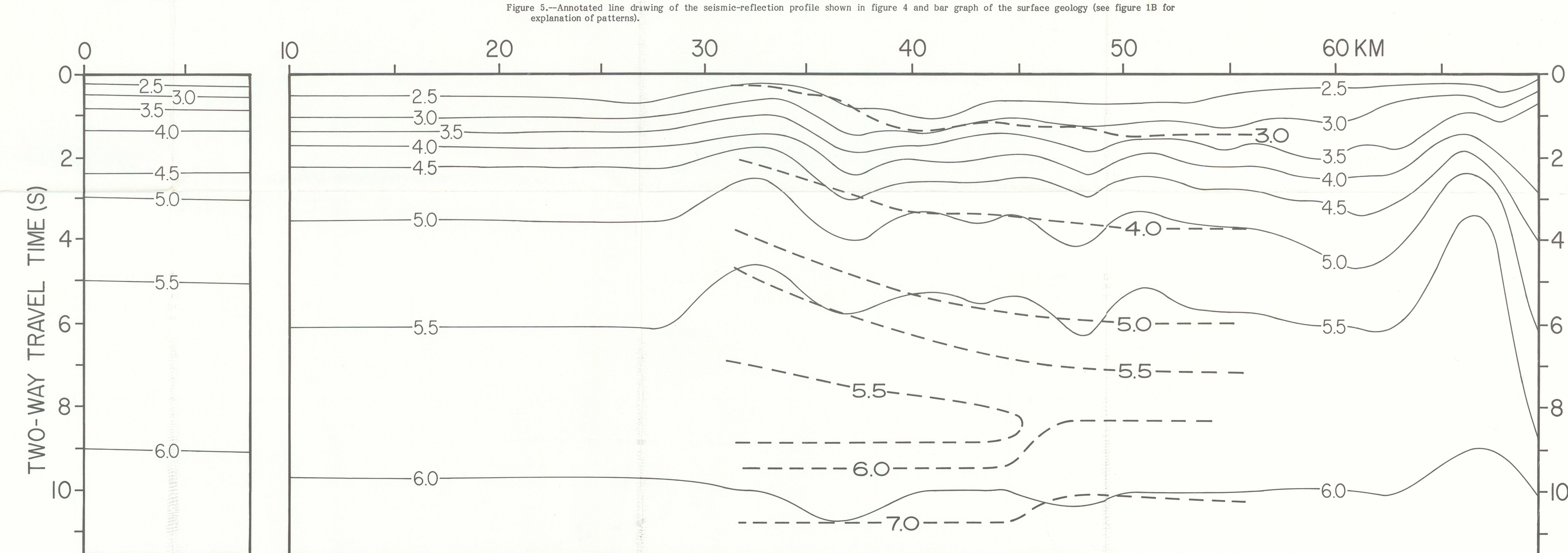


Figure 6.—Root-mean-squared velocity model for normal-moveout correction of CDP data (solid contours), and interval velocity model used for migration of stacked data (dashed contours). Numbers are in units of km/s.

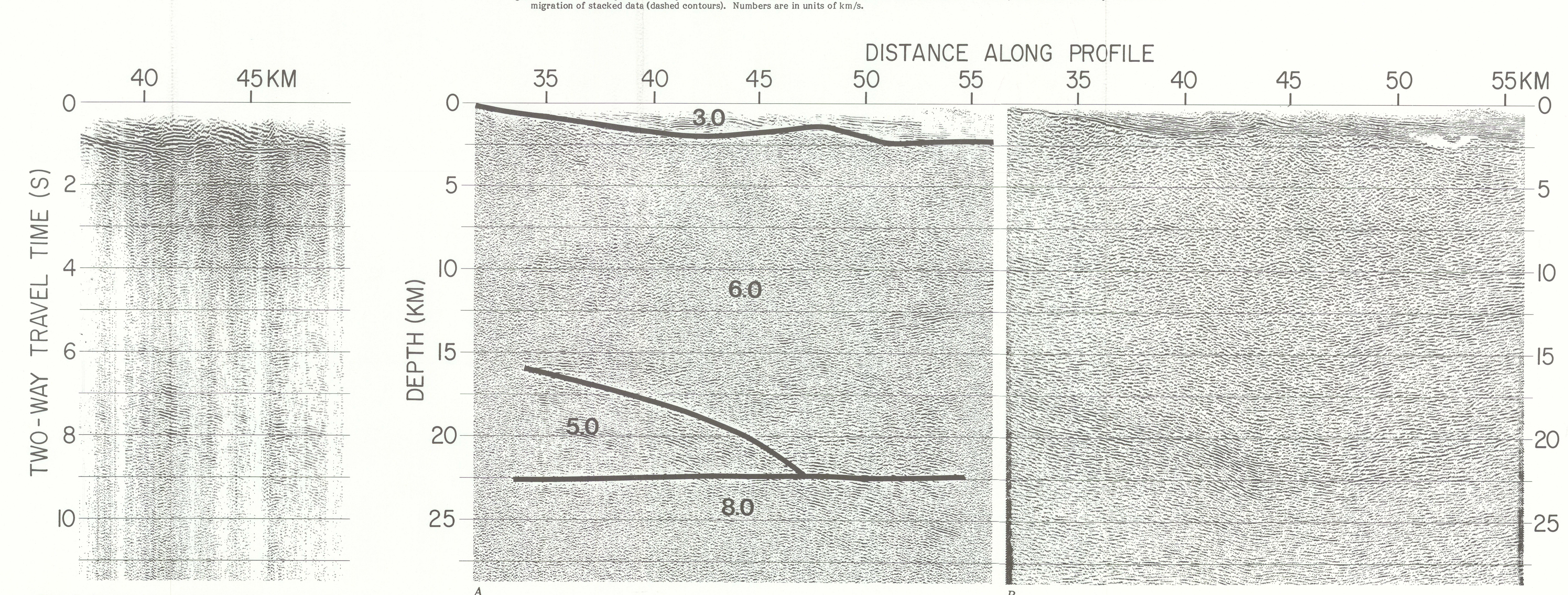


Figure 7.—Example of seismic data to which no AGC has been applied. True amplitude relationships are therefore preserved, and no additional spherical divergence correction, an exponential gain was applied from 3 to 12 s with the gain at 7.5 s relative to 3 s being 6 decibels.

Figure 8—A, Depth section of a part of the seismic-reflection profile. The velocity model shown by dashed contours in figure 6 was used for migration; the migrated time section was converted to depth using the same model as in A.